

## Re-deposition dynamics of trace $^{13}\text{C}$ in H-mode divertor conditions

M.I. Airila<sup>1</sup>, T. Makkonen<sup>2</sup>, A. Järvinen<sup>2</sup>, M. Groth<sup>2</sup>, S. Brezinsek<sup>3</sup>, J.P. Coad<sup>1</sup>, S. Jachmich<sup>4</sup>,  
A. Kirschner<sup>3</sup>, J. Likonen<sup>1</sup>, A. Meigs<sup>5</sup>, M. Rubel<sup>6</sup>, A. Widdowson<sup>5</sup> and JET-EFDA Contributors\*

*JET-EFDA, Culham Science Centre, Abingdon, UK*

<sup>1</sup> *VTT Technical Research Centre of Finland, Association EURATOM-Tekes, Finland*

<sup>2</sup> *Aalto University, Association EURATOM-Tekes, Finland*

<sup>3</sup> *Forschungszentrum Jülich, Association EURATOM-FZJ, Germany*

<sup>4</sup> *Association "EURATOM - Belgian State" Laboratory for Plasma Physics, Belgium*

<sup>5</sup> *Euratom/CCFE Fusion Association, Culham Science Centre, Abingdon, UK*

<sup>6</sup> *Association EURATOM-VR, Fusion Plasma Physics, EES, KTH, Sweden*

### Introduction

This contribution focuses on a particular local impurity transport mechanism, "walking" [1], based on re-erosion of C, which is believed to have a significant capability to accumulate impurities into remote divertor corners, possibly forming thick hydrogen-rich deposits. To this end, we revisit the JET 2004 and 2009 tracer injection experiments, in which the experimental campaigns were concluded by injecting  $^{13}\text{CH}_4$  into series of identical ELMy H-mode plasmas in the scrape-off layer at the outer divertor. The first experiment is described in detail in [1], where a consistent picture of  $^{13}\text{C}$  migration in a global scale was achieved by extensive modelling with the EDGE2D/NIMBUS code suite. However, local modelling of this experiment [2] has not yet successfully matched divertor plasma conditions, impurity emission and post-mortem measurements simultaneously. The 2009 experiment and corresponding local modelling has been reported in [3], but the modelling has been extended to employ a long-range migration model that will be described in detail in a subsequent paper. First results shown in this paper illustrate that the deposition on the entire divertor can be much better explained with the extended model.

Although the present contribution still focuses on JET results with the carbon wall, walking is a result of sputtering and therefore relevant for all impurity species. Moreover, co-deposition of hydrogen is relevant for beryllium as well. Available tracer injection data is still dominated by  $^{13}\text{C}$  as the opportunities to gather data only occur once a campaign.

The ERO code [4] provides a simulated deposition pattern on plasma-facing surfaces that is compared to post-mortem analysis results. We show that re-erosion modifies the initial deposition pattern; in typical magnetic geometries walking tends to drive impurities from the strike point stepwise towards the remote corners of the divertor. This walking is enhanced by increased target plasma temperatures and profile broadening during ELMs. Simplifying the phenomenon

\*See the Appendix of F Romanelli et al., Proc 24th IAEA Fusion Energy Conference 2012 San Diego, USA

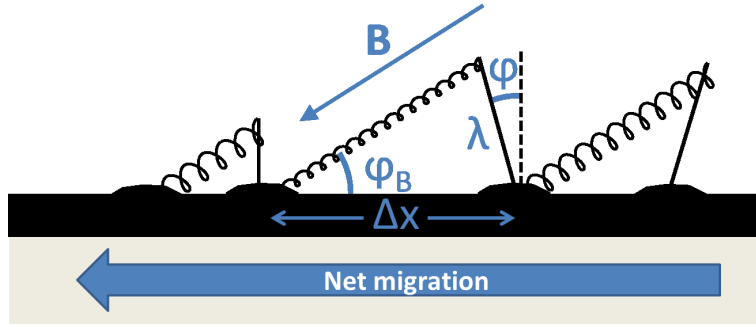


Figure 1: Under the influence of an oblique magnetic field, eroded impurities tend to “walk” to the direction where the angle between  $\mathbf{B}$  and the surface is obtuse. One step consists of the ballistic trajectory of a neutral particle across  $\mathbf{B}$  followed by the gyration of an ion along  $\mathbf{B}$  back to the surface.

into two consecutive steps – ballistic emission of neutral atoms or molecules followed by gyration of the atomic or molecular ion along  $\mathbf{B}$  – we can derive an estimate for the average step length (for the notation refer to Fig. 1):

$$\langle \Delta x \rangle = \int_0^\infty \int_0^{2\pi} \int_0^{\pi/2} \lambda \left( \sin \varphi \cos \theta - \frac{\cos \varphi}{\tan \varphi_B} \right) g(\theta, \varphi) f(\lambda) \sin \varphi d\varphi d\theta d\lambda = -\frac{2\lambda_0}{3 \tan \varphi_B}, \quad (1)$$

assuming that the distributions for the free path and emission direction of neutrals are  $f(\lambda) = \frac{1}{\lambda_0} \exp(-\lambda/\lambda_0)$  and  $g(\theta, \varphi) = \frac{1}{\pi} \cos \varphi$ , respectively. Here  $\theta$  is the polar angle of emission. This result implies a net transport into the direction where  $\mathbf{B}$  forms an obtuse angle with the surface, but estimating the walking velocity lies beyond the scope of the present paper. In a tokamak geometry  $\mathbf{B}$  is predominantly toroidal and consequently also walking steps are almost toroidal.

### Simulation model

Plasma conditions at and near the divertor targets were replicated based on Langmuir probe measurements ( $n_e$  and  $T_e$ ) with the help of the Onion-Skin Model (OSM) [5]. Integrating 1D plasma conservation equations upwards from a boundary condition at the targets, the method inherently matches the target data and provides a solid basis for local impurity modelling.

Using the OSM simulation results as the plasma background, impurity transport is calculated using the 3D Monte Carlo impurity transport code ERO [4] with the assumption that re-erosion of deposited (soft) layers is enhanced by factor 5 with respect to the substrate carbon. We use periodic boundaries in both simulation cases to describe the toroidal periodicity of the injection.

### Results

Fig. 2 shows the simulated 2D deposition pattern in the 2004 experiment and compares the deposition profiles from ERO to those from SIMS. Clear, partly overlapping deposition tails are formed from the two injection locations in one toroidal period, which explains the two measured maxima between  $-50$  and  $0$  mm. In the simulation the tails merge at the location SIMS B. A rather remarkable fraction of the injected  $^{13}\text{C}$  crosses the separatrix and forms a deposit in

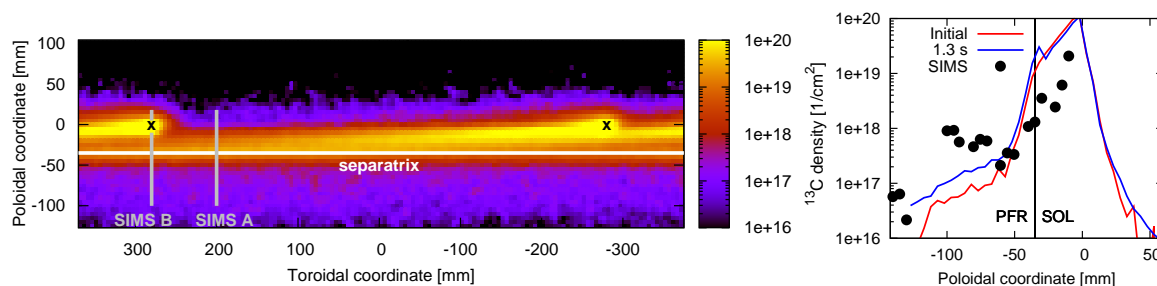


Figure 2: (Left) Simulated  $^{13}\text{C}$  deposition pattern in the 2004 tracer injection (view from inside to the vertical outer divertor). Injector locations are marked with “x”, and SIMS measurement lines are shown in grey. (Right) Toroidally averaged poloidal profiles of the deposition initially and after about 1.3 s of injection and simultaneous re-erosion compared to the measurement SIMS B [1].

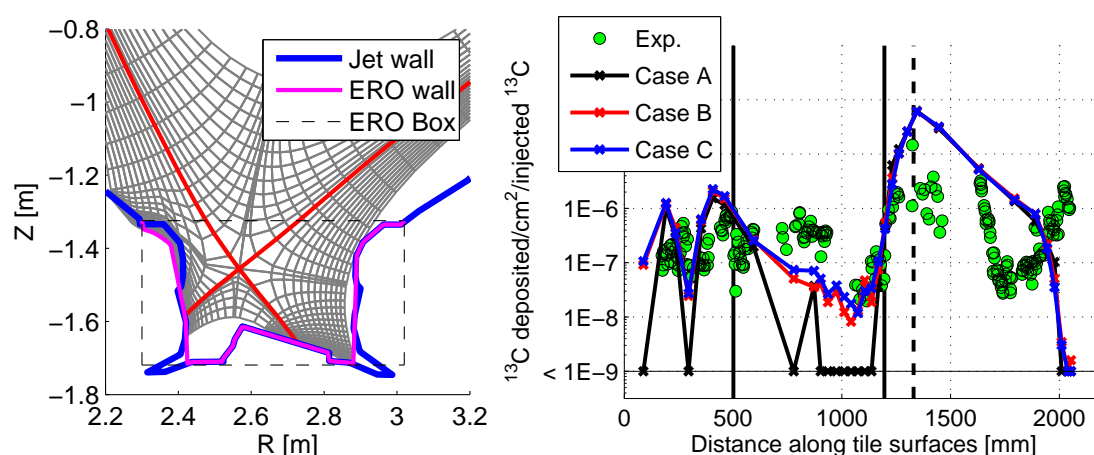


Figure 3: (Left) Calculation grid used in ERO and DIVIMP simulations of the 2009 experiment together with the simulation box of ERO and the contour of the wall used as an input in ERO. (Right) Simulation results together with experimental data [3] for three cases. Case A = initial deposition, Case B = after 50 s, Case C = after 100 s.

the PFR. We also show the toroidally averaged poloidal profile compared to the SIMS data. Although the simulation time is limited, it is already clear that re-erosion transports material preferentially into the PFR (to the left), consistently with the walking mechanism.

For the 2009 experiment we set up an ERO model that covers the entire divertor and includes a transport model outside the simulation volume. The poloidal deposition profiles in Fig. 3 illustrate that re-erosion transports deposited material from the inner divertor into the PFR (to the right), but not from the outer divertor to the PFR (due to the horizontal target geometry the expected walking direction is to the right also there).

It is not obvious whether impurity walking requires a plasma flow, which is always present when field lines cross material surfaces, or whether the magnetic geometry alone could give rise to the effect even if the flow were suppressed. To investigate the significance of the flow, we carried out a set simplified simulations in a planar surface geometry, uniform plasma, purely

poloidal magnetic field (angle of  $5^\circ$  with respect to the surface) and replacing the injection source with a narrow  $^{13}\text{C}$  marker on the surface. Following the evolution of  $^{13}\text{C}$  surface concentration distribution, with different parallel flow velocities assigned to the plasma ( $u = 0$ ,  $u = 0.01c_s$ , or  $u = c_s$ ), net transport is observed in all cases (81 to 100 % of eroded particles are deposited “downstream”, respectively, which clearly illustrates that walking is a robust effect if the field lines are sufficiently inclined). Parallel flow certainly amplifies the effect by forcing the parallel motion towards the target and thus significantly increases the locally re-deposited fraction of eroded or injected impurities.

## Conclusions

We have used post-mortem surface analysis data from JET supported with ERO modelling to explain a dominant local migration mechanism called “walking”. In general the initial deposition decays uniformly with increasing distance from the source, but the pattern can be significantly re-distributed due to re-erosion. In typical magnetic tokamak divertor geometries, re-erosion preferentially drives impurities towards divertor corners. All three available cases support the walking model: (i) 2004 outer divertor: Re-erosion produces an additional maximum in PFR (strong re-erosion at the OSP); (ii) 2009 inner divertor: Re-erosion steps spread the deposition into the PFR; (iii) 2009 outer divertor: No spreading into the PFR (against the walking direction).

More pronounced walking was demonstrated with simplified ERO simulations, showing also that the walking is enhanced by but not completely dependent on a frictional force from plasma flow that drives eroded impurities back to the target. Obviously the effect depends quite strongly on local plasma conditions and is in general relatively weak in tokamak divertors due to the predominantly toroidal magnetic field.

## Acknowledgments

This work, supported by the European Communities under the contract of Association between Euratom/Tekes, was carried out within the framework of the European Fusion Development Agreement. The views and opinions expressed herein do not necessarily reflect those of the European Commission. This work was partially funded by the Academy of Finland projects No. 134924 and 134930.

## References

- [1] J. Strachan et al., *Nuclear Fusion* **48**, 105002 (2008)
- [2] M.I. Airila et al., *Phys. Scripta* **T138**, 014021 (2009)
- [3] J. Likonen et al., *Phys. Scripta* **T138**, 014004 (2009)
- [4] A. Kirschner et al., *Nuclear Fusion* **40**, 989 (2000)
- [5] P.C. Stangeby et al., *J. Nucl. Mater.* **290–293**, 733 (2001)